Application of Multivariate Model Based on Three Simulated Sensors for Water Quality Variables Estimation in Shitoukoumen Reservoir, Jilin Province, China

JIANG Guangjia[1, 2], LIU Dianwei[1], SONG Kaishan[1], WANG Zongming[1],
ZHANG Bai[1], WANG Yuandong[1, 2]

(1. Northeast Institute of Geography and Agroecology, Chinese Academy Sciences, Changchun 130012, China;
2. Graduate University of the Chinese Academy Sciences, Beijing 100049, China)

Abstract: This study applied a multivariate model based on three simulated sensors to estimating water quality variables in Shitoukoumen Reservoir, Changchun City, Jilin Province, China, including concentration of total suspended matter, concentration of chlorophyll-*a* and non-pigment matter absorption. Two field campaigns for spectra measurements with a total of 40 samples were carried out on June 13 and September 23, 2008. The in-situ spectra were recalculated to the spectral bands and sensitivities of the instruments applied in this paper, i.e. Landsat TM, Alos and P6, by using the average method. And the recalculated spectra were used for estimating water quality variables by the single model and multivariate model. The results show that the multivariate model is superior to the single model as the multivariate model takes the combined effects of water components into consideration and can estimate water quality variables simultaneously. According to R^2 and *RMSE*, Alos is superior to other sensors for water quality variables estimation although the precision of non-pigment matter absorption inversion performed the second.

Keywords: remote sensing; inland water quality; Alos; water components absorption; absorption coefficient

1 Introduction

There are four substances that mainly influence the distribution of light underwater, including water itself, phytoplankton, nonalgal particles and colored dissolved organic matter (CDOM) (Alison and James, 2005; Prieur and Sathyendranath, 1981). And light variability determines the primary production and the structure of ecosystem in the water column (Zepp *et al*., 1998). Therefore, accurate inversion of water quality variables is significant to improve the water ecosystem and evaluate the status of water pollution.

Compared with traditional methods, remote sensing is more effective for its real-time and large-scale water quality monitoring, especially when integrating the in-situ sampling. With the development of remote sensing sensors, land satellites have widely served water quality monitoring, such as Landsat TM/ETM+, SPOT and MODIS. The components in water make different contributions to water spectrum, therefore many scholars at home and abroad estimated the water quality variables according to specific spectrum responses of water components in some wave bands (David *et al*., 2004; Hellweger *et al*., 2004); Liu *et al*., 2006; Yang *et al*., 2004. The common methods for water quality inversion were single wave band, band ratio and so on, but they can only estimate single water quality variable. Additionally, the Neural Network method is usually a ″black box″ operation, which is not easily controlled.

The main objective of this study was to inverse three variables simultaneously using three simulated sensors (Landsat TM-5, Alos and P6), including concentration of total suspended matter (C_{TSS}), concentration of chlorophyll-*a* (C_{CHL}) and non-pigment matter absorption (a_{CDM}). Non-pigment matter is the combination of nonalgal particles and colored dissolved organic matter, because they

have similar absorption properties which can be described by index model. Also, we can select the specific bands for different water quality variables in order to improve the inversion precision. Specific objectives include 1) evaluating the precision of the multivariate model applied in this paper by comparing with single model; and 2) finding out which remote sensing sensor is the best for inversion, Landsat TM, Alos or P6.

2 Study Area

Shitoukoumen Reservoir in Changchun City, Jilin Province, China, was selected as the study area, which is located between 43°51′18″–43°57′54″N and 125°43′48″–125°50′06″E. The Shuangyang River and the Chalu River flow into the reservoir in the upstream (Fig. 1). As an indispensable water source of Changchun City and Jiutai City, Shitoukoumen Reservoir is in storage of 702×10^6 m³, with a drainage area of 4 975.6 km² and a surface area of 94.2 km², respectively (Xu *et al.*, 2007b). It is situated in north temperate sub-humid continental monsoon climate zone. The mean annual temperature is 5.3℃ and annual precipitation ranges from 369.9 mm to 667.9 mm, of which 80% happens from June to September. The average annual evaporation is as high as 1 658.1 mm, which might result in drought and serious water shortage at the maximum from April to June (Xu *et al.*, 2007a).

3 Methods

Two field campaigns for spectra measurements and cor-

responding water quality parameters were carried out in 20 sampling sites on June 13 and September 23, 2008 in Shitoukoumen Reservoir. Water samples were collected at the center of reservoir to prevent the influence of bottom reflection (Fig. 1). All of them were reserved in a box with ice for laboratory analysis and inherent optical properties (IOPs) measurements.

3.1 Remote sensing reflectance measurement and processing

Remote sensing reflectance was measured with a portable ASD Fieldspec-FR spectrometer (ASD Inc.), following the Above-water Method (Tang *et al.*, 2004), with a field view of 25° and a wavelength range of 350–2500 nm at an increment of 1 nm. Radiance from water surface (L_{sw}), sky (L_{sky}) and standard white reference (L_r) were measured 10 times at each sampling site and all the measurements were made at a location with minimum shading and without the influences of reflection from superstructure, boat′s wake or associated foam patches and whitecaps (Ma *et al.*, 2006). The viewing angles from water surface at zenith angel θ and azimuth angle Φ were 40° and 135°, respectively, effectively preventing the interference of boat and the influence of direct solar radiance.

Radiance from water surface (L_{sw}) can approximately be regarded as the sum of water leaving radiance (L_w) and sky diffused radiance (L_{sky}). Therefore:

$$L_{sw} = L_w + rL_{sky} \qquad (1)$$

where r is the reflectivity of skylight at the air-water interface, which depends on wind speed, solar zenith
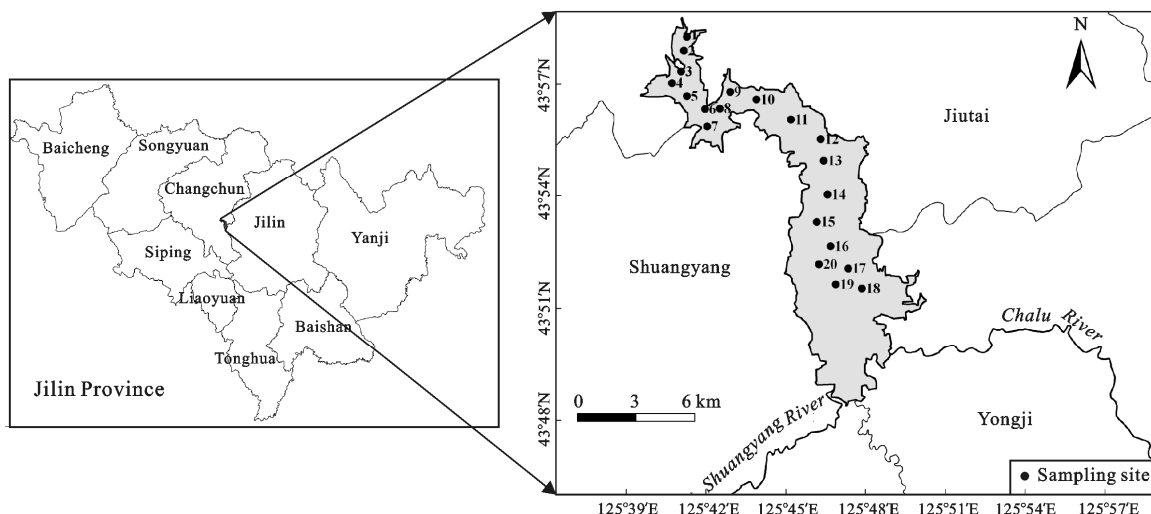

Fig. 1 Location of Shitoukoumen Reservoir in Changchun City, Jilin Province, China and sampling sites

angle, viewing geometry, *etc*. And its value ranges from 0.026 to 0.028 (Tang *et al*., 2004).

Because L_w can be easily obtained from remote sensing, remote sensing reflectance (R_{rs}) is defined as the ratio of water leaving radiance to the downwelling irradiance ($E_d(0^+)$) just above water surface (Ma *et al*., 2006). So

$$R_{rs} = L_w / E_d(0^+) \qquad (2)$$

The $E_d(0^+)$ can be expressed as:

$$E_d(0^+) = L_r \pi / \rho_r \qquad (3)$$

where ρ_r represents the reflectance of the white reference panel, which is calibrated to 30%.

Raw data were transferred into ASCII file with the software ASD ViewSpec. One spectrum was selected as the water sample reflectance according to the ratio between L_s and L_{sky}, the value of which is about 0.028 (Ma *et al*., 2006).

3.2 Inherent optical properties measurement

Spectral absorption coefficients of particles, colored dissolved material and phytoplankton were determined in the laboratory for water samples, following the measurement protocols recommended by Giulietta and James (2000). Whatman GF/F filters were used to extract total particles, including nonalgal particles and phytoplankton. The volume of water samples (V) ranged from 50 mL to 300 mL, according to the concentration of total suspended matter (C_{TSS}). The spectral absorption coefficients of total particles were calculated by the optical density which was measured by a UV2401 spectrophotometer (SHIMADZU) with 1 nm interval in the range of 350–800 nm. After that, the filters were dipped into the acetone for 30–60 minutes to extract the phytoplankton from the total particles. The way for determining the spectral absorption coefficient of nonalgal particles was the same as total particles. Subsequently, the absorption coefficient of phytoplankton was computed by subtracting absorption coefficient of nonalgal from that of total particles. For CDOM, the water sample was filtered under low vacuum on a 0.2 μm Millipore membrane, which had been dipped in the 10% diluted hydrochloric acid for 30 minutes. Milli-Q water was used as a reference. The absorbance of filtered water was measured between 200 nm and 750 nm with the same spectrophotometer. Then the absorption coefficients of CDOM were calculated with the method proposed by Bricaud *et al*. (1981).

The concentration of total particles was determined by weighting discrepancy. After four hours dried in the oven at 105℃, the Whatman GF/C filters were weighted with electronic balance and used to filtrate water samples and then dried and weighted again. The concentration was computed by the ratio of weighting discrepancy and volume of water samples filtrated. The spectrophotometric determination method was used to measure chlorophyll-*a* concentration. First filtered water samples though Whatman GF/F filter and extracted with ethanol (90%) at 80℃, then measured the absorbencies at 665 nm and 750 nm with UV2401 spectrophotometer. The chlorophyll-*a* concentrations were eventually acquired from calculation (Moed and Hallegraeff, 1978).

3.3 Inversion models

Some single or multivariate models for water quality variables estimation have been raised in previous researches (Carpenter and Carpenter, 1983; Giardino *et al*., 2001; Kabbara *et al*., 2008).

The forms of the single models are as follows (Su *et al*., 2008):

$$\log Y = c_0 + \sum_{i=1}^{k} c_i \log X_i \qquad (4)$$

$$\log Y = c_0 + \sum_{i=1}^{k} c_i X_i \qquad (5)$$

$$Y = c_0 + \sum_{i=1}^{k} c_i X_i \qquad (6)$$

where Y presents a water quality parameter; X_i is the reflectance of the ith specific spectral band, or the ith ratio of reflectance of different spectral bands, or the ith other recalculated band reflectance; c_0 and c_i are the regression coefficients.

For multivariate model,

$$\begin{bmatrix} C_{CHL_1} & C_{TSS_1} & a_{CDM_1} \\ C_{CHL_2} & C_{TSS_2} & a_{CDM_2} \\ \vdots & \vdots & \vdots \\ C_{CHLn} & C_{TSSn} & a_{CDMn} \end{bmatrix} = \begin{bmatrix} 1 & \rho_{B_1} & \rho_{G_1} & \rho_{R_1} \\ 1 & \rho_{B_2} & \rho_{G_2} & \rho_{R_2} \\ 1 & \vdots & \vdots & \vdots \\ 1 & \rho_{B_n} & \rho_{G_n} & \rho_{R_n} \end{bmatrix} \cdot \begin{bmatrix} \beta_{10} & \beta_{20} & \beta_{30} \\ \beta_{11} & \beta_{21} & \beta_{31} \\ \beta_{12} & \beta_{22} & \beta_{32} \\ \beta_{13} & \beta_{23} & \beta_{33} \end{bmatrix} \qquad (7)$$

where ρ_{Bi}, ρ_{Gi}, ρ_{Ri} are the band ratios of B/IR, G/IR and R/IR of the ith water sample, respectively; β_{ij} represents the regression coefficients, and n is the number of water quality measurements.

The multivariate model can also be expressed as:

$$Y = XM \qquad (8)$$

where *Y* is water quality variable; *X* is band ratio; and *M* is the regression coefficient.

In this study, Matlab R2007a software was used for the data processing and water quality variables modeling. The matrix operations and the least squared estimator were carried out to calculate the regression coefficient matrix of the multivariate model. The descriptive statistics for water quality variables, such as mean, variance, root mean square error, and so on, were estimated by the Origin 8.0.

4 Results

4.1 In-situ water spectra and water quality variables

The measured remote sensing reflectance spectra (350–800 nm) are shown in Fig. 2. The reflectance has been established in full spectral resolution (1 nm), so that the spectra can be recalculated to the spectral bands and sensitivities of the instruments applied (Dekker *et al*., 2001), including the Landsat TM-5, Alos and P6 in this study (Table 1). By averaging the reflectance over the entire width of spectral band as the image data, the recalculated spectra can be used for estimating water quality variables (Fig. 3).

Table 2 lists the values of water quality variables measured in June and Semptember, including C_{TSS}, C_{CHL} and a_{CDM}. The averages of C_{TSS} and a_{CDM} are higher in June than that in September, but C_{CHL} lower. And they are used to establish water quality estimation models based on the recalculated remote sensing reflectance.

Table 1 Information of different remote sensing sensors in this study

Remote sensing sensor	Wave band	Wave range (nm)	Spatial resolution (m)
Landsat TM-5	Blue (B)	450–520	30
	Green (G)	520–600	
	Red (R)	630–690	
	Infrared (IR)	760–900	
Alos	Blue (B)	420–500	10
	Green (G)	520–600	
	Red (R)	610–690	
	Infrared (IR)	760–890	
P6	Green (G)	520–590	23
	Red (R)	620–680	
	Infrared (IR)	770–860	

4.2 Water quality variables estimation by single model

Single model for estimating water quality variables was established in this study for comparing with the multivariate model. In order to choose appropriate bands for water quality variables estimation, we analyzed the correlativity of band ratio and in-situ datasets (Table 3). The B/IR band ratio of Alos shows a high correlation for

Table 2 Measured values of different water quality variables in different sampling times

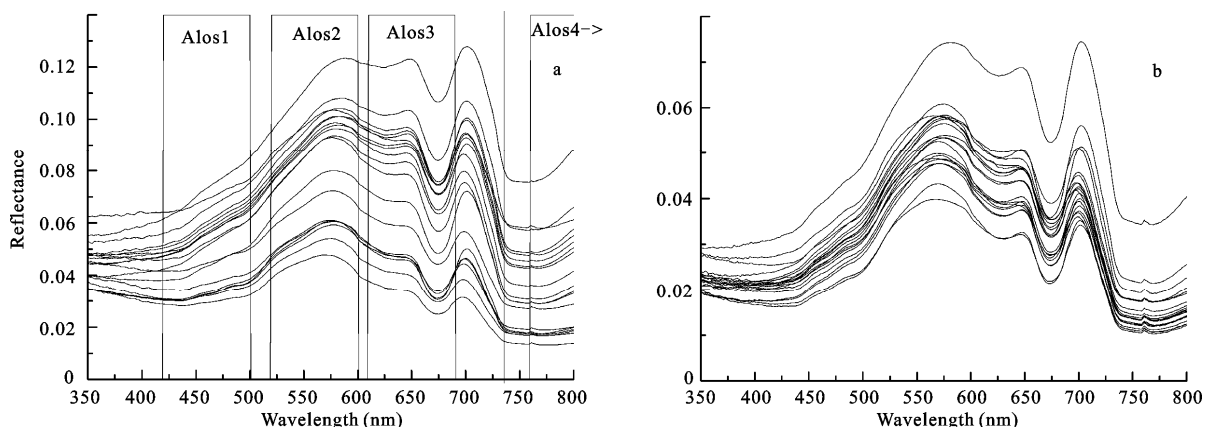| Sampling time	C_{TSS} (mg/L)		C_{CHL} (μg/L)		a_{CDM} (440nm) (1/m)	
	Range	Average	Range	Average	Range	Average
June	12.50–121.00	40.03±26.82	12.90–36.38	24.76±6.77	1.79–18.07	5.78±4.42
September	15.29–57.29	23.79±10.94	15.75–47.52	35.23±7.95	2.26–6.25	4.15±1.12

Fig. 2 In-situ remote sensing reflectance spectra in Shitoukoumen Reservoir in June (a) and September (b) 2008

Table 3 Correlation coefficients between different band ratios and water quality variables

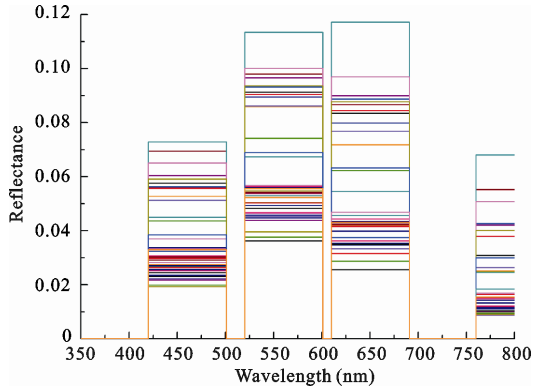| Variable	Landsat TM-5			Alos			P6	
	B/IR	G/IR	R/IR	B/IR	G/IR	R/IR	G/IR	R/IR
C_{TSS}	−0.770	−0.578	−0.579	−0.807	−0.774	−0.614	−0.781	−0.653
C_{CHL}	−0.101	−0.554	0.057	−0.214	0.046	0.037	0.016	0.003
a_{CDM}	−0.392	−0.287	−0.204	−0.444	−0.367	−0.238	−0.406	−0.274

Fig. 3 In-situ remote sensing reflectance spectra of Alos bands 1–4 spectra in Shitoukoumen Reservoir

C_{TSS} and a_{CDM}. While Landsat TM is the best for chlorophyll-*a* estimation. For P6 sensor, the correlation coefficients are the lowest.

All band ratios are highly related to C_{TSS} and the maximum correlation coefficient is at the B/IR of Alos. The max absolute correlation coefficient of a_{CDM} estimation is at the same band ratio of Alos with the value only 0.444. But for C_{CHL}, only the G/IR of Landsat TM presents high coefficient.

Water quality variables, C_{TSS}, a_{CDM} and C_{CHL}, were inversed separately by B/IR band ratio of Alos, B/IR of Alos and G/IR of Landsat TM (Fig. 4). Single models for C_{TSS}, a_{CDM} and C_{CHL} estimation were selected according to the best fitting correlation coefficient.

4.3 Water quality variables estimation by multivariate model

A total of 40 samples were used for least squared estimator of regression coefficients. The regression coefficient matrixes *M* for Alos, Landsat TM and P6 are as follows:

For Alos:

$$[C_{CHL} \ C_{TSS} \ a_{CDM}] =$$
$$[1 \ \rho_B \ \rho_G \ \rho_R] \cdot \begin{bmatrix} 65.71 & 60.89 & 4.55 \\ -52.32 & -19.94 & -2.09 \\ 37.17 & -30.98 & -4.60 \\ -21.80 & 41.86 & 7.26 \end{bmatrix} \quad (9)$$

For Landsat TM:

$$[C_{CHL} \ C_{TSS} \ a_{CDM}] =$$
$$[1 \ \rho_B \ \rho_G \ \rho_R] \cdot \begin{bmatrix} 45.41 & 63.33 & 4.03 \\ 9.39 & -68.36 & -10.79 \\ -12.53 & 8.01 & 1.95 \\ -0.82 & 37.73 & 7.37 \end{bmatrix} \quad (10)$$

For P6:

$$[C_{CHL} \ C_{TSS} \ a_{CDM}] =$$
$$[1 \ \rho_G \ \rho_R] \cdot \begin{bmatrix} 31.42 & 52.26 & 3.55 \\ 2.06 & -43.06 & -5.95 \\ -3.14 & 45.20 & 7.88 \end{bmatrix} \quad (11)$$
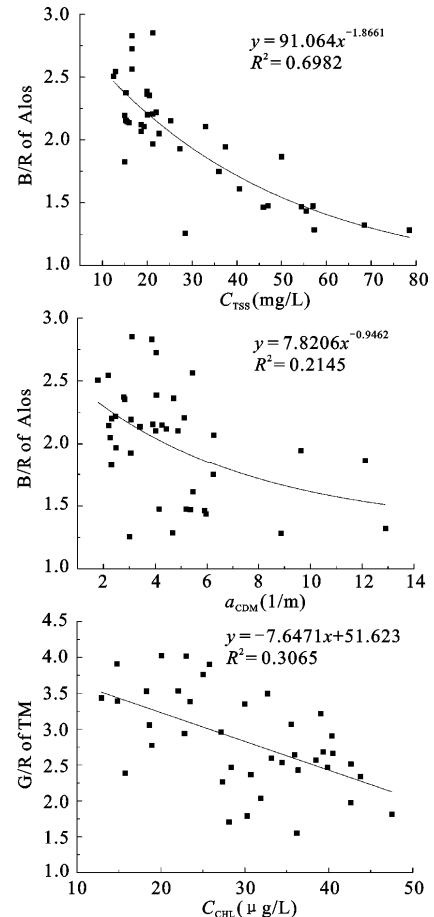

Fig. 4 Water quality variables estimated by single models

Compared with the single model, multivariate model presents higher precision and significantly less degree of dispersion around the line of equivalence as shown in Fig. 5. The results show that Alos is superior to other sensors for water quality variable estimation although the precision of a_{CDM} is the second.
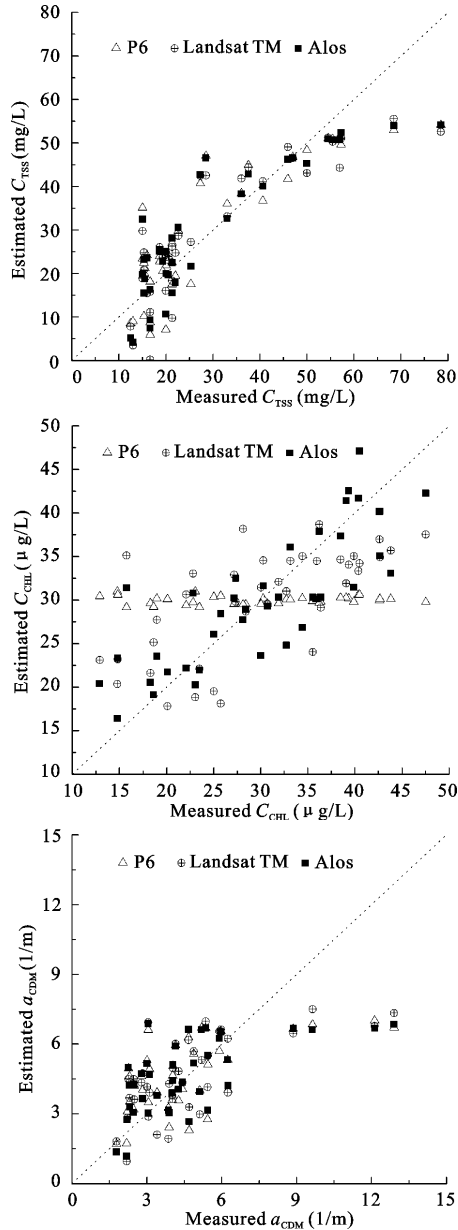

Fig. 5 Water quality variables estimated and measured
for different sensors

Table 4 demonstrates the descriptive statistics of different sensors for estimating water quality variables. The correlation efficient (R^2) and root mean square error (*RMSE*) of Alos demonstrate that it is best for water quality variables estimation, except for a_{CDM}. P6 is the lowst effective for C_{CHL} estimation. The inversion of a_{CDM} has poor accuracy among all the remote sensing sensors, which is opposite to C_{TSS} estimation.

Table 4 Descriptive statistics of different sensors
for water quality variables estimation

Variable	Landsat TM-5		Alos		P6	
	R^2	*RMSE*	R^2	*RMSE*	R^2	*RMSE*
C_{TSS}	0.750	4.26	0.766	3.98	0.746	4.31
C_{CHL}	0.443	5.11	0.652	3.19	0.003	9.14
a_{CDM}	0.420	1.45	0.374	1.57	0.356	1.61

5 Discussion

5.1 Comparison between single model and multivariate model

Single model and multivariate model are applied to estimating water quality variables in Shitoukoumen Reservoir from the simulated remote sensing sensors, including Landsat TM-5, Also and P6. The errors of the estimated parameters by multivariate model are smaller than that by single model. The comparison of the in-situ measured data and estimated data are shown in Fig. 4 and Table 4.

There are two main reasons why the multivariate model gets smaller errors in water quality estimation. Firstly, the multivariate model has an evident advantage with its integrative information for water quality variables estimation. The reflectance is determined by combined effect of the water components and every wave-band contains the information of water. All band ratios were selected in this paper to take full advantage of all the water components information. Secondly, the water quality variables could also be computed simultaneously by multivariate model. Least squared estimator was used to achieve the regression coefficient matrixes with in-situ water quality data and then the three variables were inversed. But for the single model, different specific band ratios were chosen for different variables according to the correlation coefficient.

5.2 Different sensors for water quality variables estimation

The average absorption coefficient of photosynthetic active radiation wave band (400–700 nm) is used to evaluate the contribution to total absorption of water components (Zhang *et al*., 2006; Le *et al*., 2008). Figure 6

shows the absorption ratios of different water components in June and September, including nonalgal particles, phytoplankton and CDOM.
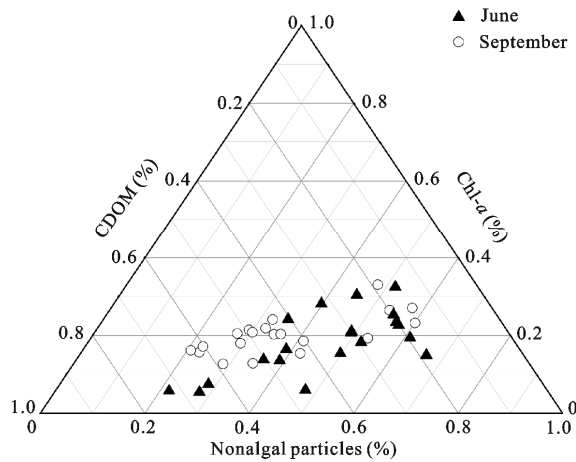

Fig. 6 Ratios of water components absorption
in June and September

The nonalgal particles and CDOM in June and September were dominant in the total absorption of water components, and the absorption of phytoplankton varied slightly but performed the last. In June, the absorption ratio of CDOM changed from 0.16 to 0.72 and nonalgal particles from 0.22 to 0.66. But for phytoplankton, the maximum was only 0.32 which accounted for only less than one-third of the total absorption. In September, CDOM contributed greatly to the total absorption of water components with the average ratio 0.43. The absorption ratio of nonalgal particles declined relatively, changing from 0.15 to 0.63.

The absorption spectra of nonalgal particles and CDOM in the range of 350–700 nm decrease with wavelength and they dominantly affect water reflectance in the blue band in Shitoukoumen Reservoir. Compared with P6 and Landsat TM, Alos sensor has broad range of blue band and contains 440 nm which is the absorption peak for phytoplankton. It maybe contributes to the high precision for the estimation of concentration of chlorophyll-*a*. Another superior of the Alos sensor lies in its higher spatial resolution. For the inland water, higher spatial and temporal resolution is imperative for improving the precision of water quality variables estimation in future due to the influence of land use/cover changes (Pan and Ma, 2008). So Alos is the best sensor for water quality variables estimation.

6 Conclusions

Based on the two campaigns of field spectra measurements with a total of 40 samples in Shitoukoumen Reservoir, three water quality variables, concentration of total suspended matter (C_{TSS}), concentration of chlorophyll-*a* (C_{CHL}) and non-pigment matter absorption (a_{CDM}), were estimated by the single model and multivariate model.

The water surface reflectance depends on the mixture of suspended mater, phytoplankton, CDOM and water itself. The multivariate model could take full advantage of all the water components information and yield more accurate water variables estimation results. Also, the water quality variables could be computed simultaneously.

The absorption of nonalgal particles and CDOM were dominant in Shitoukoumen Reservoir, which influenced water surface reflectance in the blue band. Compared with Landsat TM and P6, Alos was the best sensor for water quality variables estimation. It had broad range of blue band and higher spatial resolution.

However, the sensors were simulated by in-situ spectrum datasets in this paper. And the water quality variables should be mapped utilizing satellite images for long term monitoring in the future.

Acknowledgements

References

Alison B B, James N K, 2005. The relative importance of chlorophyll and colored dissolved organic matter (CDOM) to the prediction of the diffuse attenuation coefficient in shallow estuaries. *Estuaries and Coasts*, 28(5): 643–652. DOI: 10.1007/BF02732903

Bricaud A, Morel A, Prieur L, 1981. Absorption by dissolved organic matter of the sea (yellow substance) in the UV and visible domain. *Limnology and Oceanography*, 26(1): 43–53.

Carpenter D J, Carpenter S M, 1983. Modeling inland water quality using Landsat Data. *Remote Sensing of Environment*, 13: 345–352. DOI: 10.1016/0034-4257(83)90035-4

David Doxaran, Samantha J L, Jean-Marie Froidefond, 2004. Mapping tidal and seasonal movements of the maximum turbidity zone in estuarine waters from remotely sensed (SPOT,

LANDSAT) data. A semi-empirical approach. *EARSeL eProceedings*, 3(1): 54–68.

Dekker A G, Vos R J, Peters S W M, 2001. Comparison of remote sensing data, model results and in situ data for total suspended matter (TSM) in the southern Frisian lakes. *The Science of the Total Environment*, 268: 197–214. DOI: 10.1016/S0048-9697 (00)00679-3

Giardino C, Pepe M, Brivio P A *et al*., 2001. Detecting chlorophyll, Secchi disk depth and surface temperature in a sub-alpine lake using Landsat imagery. *The Science of the Total Environment*, 268: 19–29. DOI: 10.1016/S0048-9697(00)00692-6

Giulietta S F, James L M, 2000. Ocean optics protocols for satellite ocean color sensor validation, Revision 2. *NASA/TM-2000-209966*, Goddard Space Flight Space Center.

Hellweger F L, Schlosser P, Lall U *et al*., 2004. Use of satellite imagery for water quality studies in New York Harbor. *Estuarine Coastal and Shelf Science*, 61(3): 437–448. DOI: 10.1016/ j.ecss.2004.06.019

Kabbara N, Benkhelil J, Awad M *et al*., 2008. Monitoring water quality in the coastal area of Tripoli (Lebanon) using high-resolution satellite data. *ISPRS Journal of Photogrammetry and Remote Sensing*, 63(5): 488–495. DOI: 10.1016/j.isprsjprs.20-08.01.004

Le Chengfeng, Li Yunmei, Zha Yong *et al*., 2008. Seasonal variation of in water constituents′ absorption properties in Meiliang Bay of Taihu Lake. *Environmental Science*, 9: 2448–2455. (in Chinese)

Liu Dianwei, Zhang Bai, Song Kaishan *et al*., 2006. *Study on Regional Landscape Information of Remote Sensing*. Beijing: Science Press. (in Chinese)

Ma R H, Tang J W, Dai J F, 2006. Bio-optical model with optimal parameter suitable for Taihu Lake in wager colour remote sensing. *International Journal of Remote Sensing*, 27(19): 4305–4327. DOI: 10.1080/01431160600857428

Moed J R and Hallegraeff G M, 1978. Some problems in the estimation of chlorophyll-*a* and phaeopigments pre- and post-acidification spectrophotometric measurements. *International Review of Hydrobiology*, 63(6): 787–800. DOI: 10.1002/iroh.197-80630610

Pan Delu, Ma Ronghua, 2008. Several key problems of lake water quality remote sensing. *Journal of Lake Sciences*, 20(2): 139–144. (in Chinese)

Prieur L, Sathyendranath S, 1981. An optical classification of coastal and oceanic waters based on the specific spectral absorption curves of phytoplankton pigments, dissolved organic matter, and other particulate materials. *Limnology and Oceanography*, 26: 671–689.

Su Y F, Liou J J, Hou J C *et al*., 2008. A multivariate model for coastal water quality mapping using satellite remote sensing images. *Sensors*, 8: 6321–6339. DOI: 10.3390/s8106321

Tang Junwu, Tian Guoliang, Wang Xiaoyong *et al*., 2004. The methods of water spectra measurement and analysis I: Above-Water Method. *Journal of Remote Sensing*, 8(1): 37–44. (in Chinese)

Xu Jingping, Zhang Bai, Lin Yu *et al*., 2007a. Estimating total suspended sediments concentrations and transparency with hyper-spectral reflectance in Shitoukoumen Reservoir, Jilin Province. *Journal of Lake Sciences*, 19(3): 269–274. (in Chinese)

Xu J P, Zhang B, Song K S *et al*., 2007b. Simplified bio-optical modelling of concentrations of total suspended matter in a turbid inland water condition. *SPIE*. 6752: 67521J1–67521J9. DOI: 10.1117/12.760493

Yang Yipeng, Wang Qiao, Wang Wenjie *et al*., 2004. Application and advances of remote sensing techniques in determining water quality. *Geography and Geo-Information Science*, 20(6): 6–12. (in Chinese)

Zepp R G, Callaghan T V, Erickson D J, 1998. Effects of enhanced solar ultraviolet radiation on biogeochemical cycles. *Journal of Protochemistry Photobiology B*: *Biology*, 46: 69–82. DOI: 10.1016/S1011-1344(98)00196-9

Zhang Yunlin, Qin Boqiang, Yang Longyuan, 2006. Spectral absorption coefficients of particulate matter and chromophoric dissolved organic matter in Meiliang Bay of Taihu Lake. *Acta Ecologica Sinica*, 26(12): 3969–3979. (in Chinese)